Nonlinear Dynamics **4:** 655–670, 1993.

Nonlinear and Chaotic Oscillations of a Constrained Cantilevered Pipe Conveying Fluid: A Full Nonlinear Analysis

M. P. PAÏDOUSSIS and C. SEMLER
Department of Mechanical Engineering, McGill University, 817 Sherbrooke St. West, Montreal, Québec, H3A 2K6, Canada

(Received: 19 March 1992; accepted 26 August 1992)

Abstract. In this paper, the planar dynamics of a nonlinearly constrained pipe conveying fluid is examined numerically, by considering the full nonlinear equation of motions and a refined trilinear-spring model for the impact constraints – completing the circle of several studies on the subject. The effect of varying system parameters is investigated for the two-degree-of-freedom ($N = 2$) model of the system, followed by less extensive similar investigations for $N = 3$ and 4. Phase portraits, bifurcation diagrams, power spectra and Lyapunov exponents are presented for a selected set of system parameters, showing some rather interesting, and sometimes unexpected, results. The numerical results are compared with experimental ones obtained previously. It is found that in the parameter space that includes N, there exists a subspace wherein excellent qualitative, and reasonably good ($N = 2$) to excellent ($N = 4$) quantitative agreement with experiment. In the latter case, excellent agreement is not only obtained in the threshold flow velocities (u) for the key bifurcations, but the inclusion of the nonlinear terms improves agreement with experiment in terms of amplitudes of motion and by capturing features of behaviour not hitherto predicted by theory.

Key words: Fluidelasticity, stability, nonlinear, chaos.

1. Introduction

The linear and nonlinear dynamics of pipes conveying fluid has been studied quite extensively, both theoretically and experimentally, over the past thirty years. In a recent survey of the subject [1], over two hundred papers on various aspects of the problem were reviewed.

In recent years, increasing attention has been devoted to nonlinear aspects of the dynamical behaviour of the system; notable contributions were made by Holmes [2], Lundgren *et al.* [3], Rousselet and Herrmann [4] and Bajaj *et al.* [5]. From these and several other studies, it is clear that the basic system of a pipe conveying fluid and variants thereof are capable of displaying an extremely rich and variegated dynamical behaviour. Thus, the pipe conveying fluid is fast becoming a premier paradigm in dynamics, on a par with, but richer than, the classical problem of a column subjected to compressive loading [1].

In the past three years, some interest was shown to the question of whether this system is capable of displaying chaotic behaviour. Variants of the basic system were considered, modified to include strong nonlinear forces, known to be conducive to chaos. Thus, Tang and Dowell [6] considered a cantilevered pipe with an inset steel strip and equispaced magnets on either side, buckling the pipe into one or the other potential well thus generated. Once the flow velocity is sufficiently above the threshold for flutter about the buckled state, chaotic motions were shown to be possible. Another variant of the basic system was studied by Païdoussis and Moon [7], involving motion-limiting restraints on which the cantilevered pipe would impact, once the post-Hopf limit-cycle motion becomes sufficiently large as the flow velocity is increased. It was shown, both theoretically and experimentally, that chaotic oscillations occur at sufficiently high flow velocities. This, by the way, was the first closely-knit theoretical-

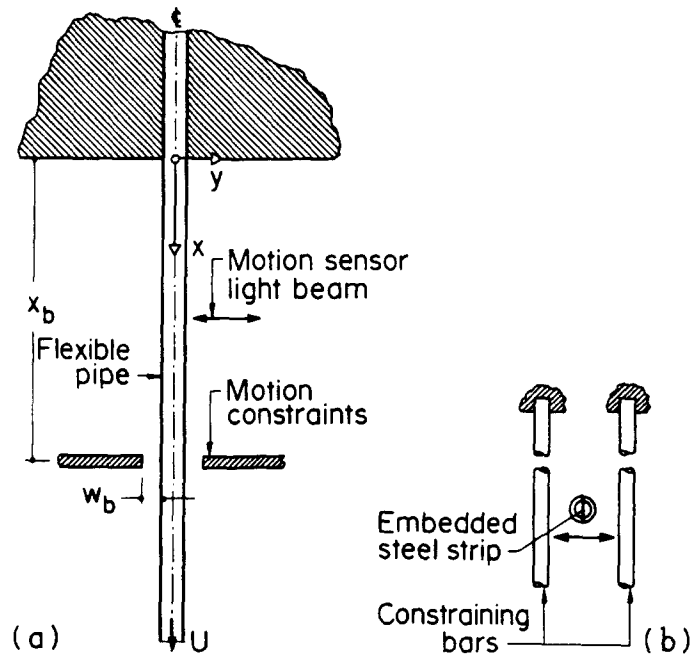

Fig. 1. (a) Schematic of the system; (b) scheme for achieving planar motions with steel strip embedded in the pipe, also showing motion constraining bars.

experimental study of chaotic dynamics of an *autonomous* mechanical system.

In the experiments [7], motions were made to be planar by embedding a steel strip into the flexible pipe. The motion-limiting restraints were parallel bars on either side of the pipe, much stiffer than the pipe itself (Figure 1); hence, a good representation of the stiffness of these constraints was by a trilinear spring: zero stiffness in the gap, and a large stiffness once contact with the restraining bars was made. In the theoretical component of this study three principal idealizations were introduced: (i) because the constraining bars were not far apart and the amplitude of motion is therefore not large, the linearized equations of motion [8], were utilized, apart from the nonlinear impact force term; (ii) a two-mode Galerkin discretization of the equations of motion was used for analysis; (iii) the trilinear spring was idealized by a cubic one, which has the advantage of being represented by an analytic function, hence permitting the calculation of Lyapanov exponents – thereby being able to prove conclusively that the chaotic-looking oscillations obtained numerically, after a period-doubling cascade, were indeed chaotic. Despite these idealizations, the correspondence between theoretical and experimental results was remarkably close qualitatively; but, quantitatively, there remained a fair margin for possible improvement. The problem was further studied theoretically with the same equations of motion by Païdoussis *et al.* [9], and the route to chaos more clearly defined.

One of the practical limitations associated with the analytical model utilized in [7] and [9] was the following: it was not possible to undertake numerical simulations with the correct (high) value of impact stiffness (and its equivalent cubic-stiffness counterpart) and the correct axial location of the impact constraint, for the solution would then diverge ("blow up" in common language). This was attributed to the inability of the two-degree-of-freedom approximation to represent the physical system. Nevertheless, parametric studies showed that,

as these parameters were varied and were made to approach the experimental ones, short of blowing up, the qualitative dynamics remained the same; so, this aspect was not considered to be of undue concern.

Analysis of typical experimental signals yielded an estimate for the fractal dimension of 3.2 in the chaotic regime [10], suggesting that, although two-degree-of-freedom (d.o.f.) modelling may be reasonable, four or five d.o.f. models may be necessary to capture all essential features of the dynamics. This idea was pursued by Païdoussis *et al.* [11], still utilizing the linearized basic equations of motion, but (i) with the number of degrees of freedom, N, in the discretization varied between two and seven, (ii) with a modified trilinear spring model for the impact restraints. It was found that for $N > 2$ it was possible to do simulations with the correct location of the restraint and value of the impact stiffness, without the solution blowing up. Furthermore, with $N = 4$ and 5, excellent agreement could be obtained between theoretical and experimental threshold flow velocities for the Hopf and period-doubling bifurcations, as well as for the onset of chaos: of the order of 10% or better.

Although better agreement between theory and experiment could hardly be expected, it was nevertheless decided to undertake the present study, which completes the circle of these studies by examining the effect of other than restraint-related nonlinearities in the equations of motion on the dynamics of the system – even when the overall amplitudes are not excessively large. Hence, the full nonlinear equations of motion will be utilized and the results compared to those in the foregoing studies. Some rather interesting and unexpected results have been obtained, as the reader will see in what follows.

2. The Analytical Model

2.1. The Equation of Motion

The system under consideration consists of a tubular beam of length L, internal cross-sectional area A, mass per unit length m, flexural rigidity EI and coefficient of Kelvin–Voigt damping a, conveying a fluid of mass M per unit length with an axial velocity U. The pipe is assumed to be initially along the x-axis (in the direction of gravity) and to oscillate in the (x, y) plane; free motions of the pipe are restrained by motion-limiting constraints as shown in Figure 1.

The nonlinear equation of motion of a vertical cantilevered pipe [3, 12] was modified to take into account the presence of motion limiting restraints [9]; for U not varying with time, it can be written as

$$EI\,(y'''' + a\dot{y}'''') + 2MU\dot{y}' + MU^2y'' - (m+M)\,g(L-s)\,y'' + (m+M)gy' + (m+M)\,\ddot{y} + N_1(y) + N_2(y) = 0\,, \tag{1}$$

where

$$\begin{aligned} N_1(y) &= F(y)\,\delta(s - s_b)\,, \\ N_2(y) &= 2MU\dot{y}'\,y'^2 + y''\,y'^2\left[MU^2 - \tfrac{3}{2}\,(m+M)\,g(L-s)\right] \\ &\quad + \tfrac{1}{2}\,g\,(m+M)\,y'y'^2 + EI\,(y''''y'^2 + 4y'y''y''' + y''^3) \\ &\quad - y''\left[\int_s^L \int_0^s (m+M)\,(\dot{y}'^2 + y'\ddot{y}')\,\mathrm{d}s\,\mathrm{d}s + \int_s^L (2MU\dot{y}'\dot{y}' + MU^2y'y'')\,\mathrm{d}s\right] \\ &\quad + y'\int_0^s (m+M)\,(\dot{y}'^2 + y'\ddot{y}')\,\mathrm{d}s\,; \end{aligned}$$

$F(y)$ is the nonlinear force on the restraint due to impact, and $\dot{(\ )}$ and $(\ )'$ denote the derivative with respect to time, t, and the curvilinear coordinate along the centreline of the pipe, s, respectively. In equation (1), $y(s,t)$ is the lateral deflection of the pipe, δ is the Dirac delta function and g is the acceleration due to gravity. Thus, in this case, the nonlinearities in the equation of motion are not only associated with the motion constraints but also with flow-dependent, gravitational and flexural terms. Therefore, equation (1) is also valid for large amplitude motions.

Introducing next the same nondimensional quantities as in the linear case,

$$\xi = \frac{s}{L}, \quad \eta = \frac{y}{L}, \quad \tau = \left(\frac{EI}{m+M}\right)^{\frac{1}{2}} \frac{t}{L^2}, \quad \alpha = \left(\frac{EI}{m+M}\right)^{\frac{1}{2}} \frac{a}{L^2},$$
$$u = \left(\frac{M}{EI}\right)^{\frac{1}{2}} UL, \quad \gamma = \frac{m+M}{EI} L^3 g, \quad \beta = \frac{M}{m+M}, \quad f(\eta) = \frac{F(y)L^3}{EI}, \tag{2}$$

and removing the nonlinear inertial terms by a perturbation method [13], equation (1) may be rewritten in dimensionless form as follows:

$$\alpha\dot{\eta}'''' + \eta'''' + 2u\sqrt{\beta}\dot{\eta}' + \eta''\left[u^2 - \gamma(1-\xi)\right] + \gamma\eta' + \ddot{\eta} + N_3(\eta) + N_4(\eta) = 0\,, \tag{3}$$

where $\dot{(\ )}$ and $(\ )'$ are now derivatives with respect to nondimensional ξ and τ, and

$$\begin{aligned}
N_3(\eta) &= f(\eta)\,\delta(\xi - \xi_b)\,,\\
N_4(\eta) &= 2u\sqrt{\beta}\dot{\eta}'\eta'^2 + \eta''\left[u^2 - \tfrac{3}{2}\gamma(1-\xi)\right]\eta'^2 - \tfrac{1}{2}\gamma\eta'^3 + 3\eta'\eta''\eta''' + \eta''^3\\
&\quad + \eta'\int_0^{\xi}\left\{\dot{\eta}'^2 - 2u\sqrt{\beta}\eta'\dot{\eta}'' - \eta'\eta'''\left[u^2 - \gamma(1-\xi)\right] + \eta''\eta''''\right\}\mathrm{d}\xi\\
&\quad - \eta''\int_{\xi}^{1}\int_0^{\xi}\left\{\dot{\eta}'^2 - 2u\sqrt{\beta}\,\eta'\dot{\eta}'' - \eta'\eta'''\left[u^2 - \gamma(1-\xi)\right] + \eta''\eta''''\right\}\mathrm{d}\xi\mathrm{d}\xi\\
&\quad - \eta''\int_{\xi}^{1}\left\{-\gamma\eta'^2 + 2u\sqrt{\beta}\,\eta'\dot{\eta}' + u^2\eta'\eta'' + \eta''\eta'''\right\}\mathrm{d}\xi\,.
\end{aligned}$$

2.2. DISCRETIZATION

The infinite dimensional model is discretized by Galerkin's technique, with the cantilever beam eigenfunctions, $\phi_r(\xi)$, being used as a suitable set of base functions and $q_r(\tau)$ being the corresponding generalized coordinates; thus,

$$\eta(\xi,\tau) = \sum_{r=1}^{N} \phi_r(\xi)\, q_r(\tau)\,. \tag{4}$$

Substituting expression (4) into (3), multiplying by $\phi_i(\xi)$ and integrating from 0 to 1, leads to

$$\ddot{q}_i + c_{ij}\dot{q}_j + k_{ij}q_j + \alpha_{ijkl}\,q_jq_kq_l + \beta_{ijkl}\,q_jq_k\dot{q}_l + \gamma_{ijkl}\,q_j\dot{q}_k\dot{q}_l = 0, \tag{5}$$

where c_{ij}, k_{ij}, α_{ijkl}, β_{ijkl} and γ_{ijkl} are coefficients computed from the integrals of the eigenfunctions $\phi_i(\xi)$, analytically [8] or numerically [14]; repeated indices implicitly follow the summation convention.

For purposes of numerical simulation, equation (5) is reduced to its first-order form,

$$\begin{Bmatrix} \dot{q} \\ \dot{p} \end{Bmatrix} = \begin{bmatrix} 0 & I \\ -K & -C \end{bmatrix} \begin{Bmatrix} q \\ p \end{Bmatrix} + \{g\,(q,p)\}\ , \tag{6}$$

i.e.

$$\dot{y} = [A]\ y + g(y)\ , \tag{7}$$

where $p_i = \dot{q}_i$, g is a third order polynomial function, and $[A] = [A(u, \gamma, \beta)]$ is a $2N \times 2N$ matrix. In equation (6), $\{q\}$ and $\{p\}$ are the generalized displacement and velocity vectors, so that the deflection of the pipe and its velocity at any point ξ may be expressed easily as

$$\eta(\xi,\tau) = \sum_{r=1}^{N} \phi_r(\xi) q_r(\tau), \quad \dot{\eta}(\xi,\tau) = \sum_{r=1}^{N} \phi_r(\xi)\ p_r(\tau)\ .$$

2.3. Modelling of the Impact and Damping Forces

Various mathematical models may be used to represent properly the impact forces. The first approximation used by Païdoussis *et al.* [7,9] was to model the restraining forces by a cubic spring, i.e. $f(\eta) = \kappa\eta^3$. A more realistic representation was that utilized by Païdoussis *et al.* [11] involving a 'smoothened' trilinear spring model, $f(\eta) = \kappa_n\{\eta - 0.5(|\eta + \eta_{bn}| - |\eta - \eta_{bn}|)\}^n$. This enables to represent adequately the free gap (in which the constraints are zero) and to smoothen the sharp discontinuity at $|\eta| = |\eta_b|$. Here, the 'cubic' ($n = 3$) trilinear model is chosen, $\kappa_3 = 5.6 \times 10^6$ and $\eta_{b3} = 0.044$, to represent the experimental constraints; the force-displacement curves of the real and the idealized constraints are shown in Figure 2(a,b). From Figure 2(a), the approximation of the cubic spring with $\kappa = 100$ seems appropriate. However, the impact forces are very small. Comparing with curves where κ is larger (Figure 2(b)) emphasizes the inadequacy of the cubic-spring model.

Païdoussis *et al.* [9] took the value of $\kappa = 100$ to overcome some numerical problems, since with values closer to the experimental ones the numerical scheme diverged. The results obtained with such a 'soft' spring were sometimes quantitatively unrealistic: e.g., the displacement of the pipe was in some cases greater than the length of the pipe itself. Nevertheless, calculations with $\kappa = 10^3$ showed that the amplitudes became more reasonable, while the critical flow velocities for the various bifurcations did not change appreciably; hence $\kappa = 100$ was used for computational convenience. As mentioned in the Introduction, the non-convergence of the solution with the more physically realistic values of $\kappa = \mathcal{O}(10^5)$ was attributed to the two-degree-of-freedom model being insufficient to physically represent the real system.

In the present paper, the nondimensional stiffness chosen for the cubic spring representation is $\kappa = 10^5$, and the idealized curve is very close to the experimental one (Figure 2), while for the trilinear model, $\kappa_3 = 5.6 \times 10^6$ and $\eta_{b3} = 0.044$.

As in previous work the dissipative forces will be modelled in two ways: either as a simple viscoelastic dissipation with $\alpha = 5 \times 10^{-3}$, or as a more realistic viscous damping representation with the individual modal logarithmic decrements, δ_j, corresponding to the experimentally measured values [7, 11]: $\delta_1 = 0.028$, $\delta_2 = 0.081$, $\delta_3 = 0.144$, and $\delta_4 = 0.200$ linearly extrapolated.

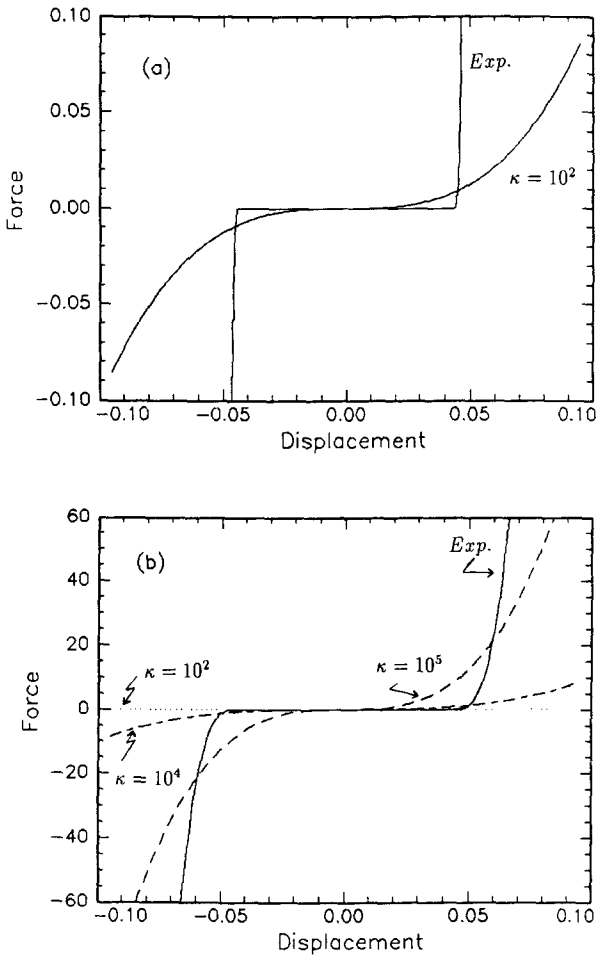

Fig. 2. Force-displacement curves for different spring stiffness κ; *Exp.* represents the experimental curve.

3. Results

3.1. Calculations to be Performed and Objectives

In what follows, results will be presented with $N = 2, 3$ and 4, with both the cubic and smoothened trilinear model for the constraints. Throughout, the results will be compared with those of the foregoing studies [7, 9, 11]. In this respect it ought to be recalled that it was shown that the $N = 2$ model is reasonably good, in terms of linear dynamics, provided that $\beta < 0.3$ [15].

The experimental parameters to which the theoretical results will ultimately be compared were selected to be $\gamma = 26.75, \beta = 0.213, \xi_b = 0.65, \eta_b = y_b/L = 0.055$ (Figure 1), $\kappa = 10^5$ for a true trilinear-spring representation and the experimental δ_j. For these parameters, the experimental nondimensional threshold flow velocities for the Hopf and first period-doubling bifurcations and for the onset of chaos were

$$u_H = 8.04, \quad u_{pd} = 8.43, \quad u_{ch} = 8.72\,, \tag{8}$$

respectively, $\pm 5\%$.

The main aim of the calculations is to explore the effect on the dynamics of the nonlinear terms in the unconstrained equation of motions. For that reason, calculations with the same parameters as those utilized, e.g., by Païdoussis *et al.* [9] were also sometimes used – rather than the experimental values: i.e., $\beta = 0.2$, $\gamma = 10$, $\alpha = 5 \times 10^{-3}$, $\kappa = 100$ and $\xi_b = 0.82$.

Throughout, solutions of equation (7) were obtained by using a fourth order Runge–Kutta integration algorithm, with a step size of 0.005 and different initial conditions (although in most cases they were $y_1(0) = 0.1$, $y_j(0) = 0, j > 1$). The results are presented in the form of bifurcation diagrams, phase portraits, power spectra and Lyapunov exponents.

3.2. Two–Degree–of–Freedom Model ($N = 2$)

3.2.1. $N = 2$ and Cubic-Spring Restraints

To check the numerical scheme, the case $\kappa = 100$ with no other nonlinear terms was investigated first with the same parameters as Païdoussis *et al.* [9]: $\beta = 0.2$, $\gamma = 10$, $\xi = 0.82$ and $\alpha = 5 \times 10^{-3}$. Chaos was found to occur at $u = 8.03$ after the classical sequence of period-doubling bifurcations. However, when the intrinsic nonlinear terms [represented by $N_4(\eta)$ in equation (3)] were added, no chaotic motion could be found, even for higher flow velocities; the nonlinearities of the pipe evidently 'kill' the big amplitudes, reducing the motion of the pipe to simple oscillations! Hence, the system becomes much more stable, from a physical and from a numerical point of view.

Theoretical results were then obtained for parameter values as in the experiments, as given in Section 3.1, and with the full nonlinear equation of motion. It is of interest that computations *can* now be carried out with the correct κ without the solution blowing up. This shows that one of the problems (the value of κ) encountered previously and thought to be related to the $N = 2$ modelling is in fact seen to be related to the previous neglect of nonlinear terms; however, a second problem, related to ξ_b remains: it is only possible to find chaotic oscillations provided ξ_b is sufficiently large, as compared to the experimental $\xi_b = 0.65$.

Indeed, for $\xi_b = 0.75$, after the Hopf bifurcation, a pitchfork bifurcation, followed by a series of period-doubling bifurcations, arises, leading to chaotic motions. Sample results are shown in Figure 3 for various values of u. At $u = 7.35$, a Hopf bifurcation occurs, leading to periodic oscillations (Figure 3(a)). A new periodic orbit is created through a pitchfork bifurcation, at $u = 9.22$, which breaks the 'symmetry' of the system (Figure 3(b)); mathematically, this comes from the crossing of a Floquet multiplier associated with the periodic trajectory, with the unit circle at $+1$ [9, 16]. Physically, the system oscillates around a newly generated steady-state. Finally, the period-doubling bifurcation is clearly visible at $u = 10.2$ (Figure 3(c)) and at $u = 10.295$ (Figure 3(d)). For $u > 10.35$, the motion becomes narrow-band chaotic, and wide-band chaotic at $u > 10.38$ (Figure 3(e,f)). From a physical point of view, the mechanism leading to chaos is related to the interaction of limit-cycle motion and potential wells associated with divergence of the pipe at the constraints.

In all the results presented in Figure 3, it should be noted that the displacement amplitudes are now quite reasonable, the tip amplitude being of the same order of magnitude as the gap to the constraint, unlike the results obtained previously [7,9].

All these characteristics can be observed either in the phase-plane portraits or in the corresponding power spectra (chaotic oscillations being associated with a wide frequency band). Notice, however, that the main frequency is still discernible at $u = 10.4$ (Figure 3(i)).

The results are summarized in two bifurcation diagrams where the maximum tip displace-

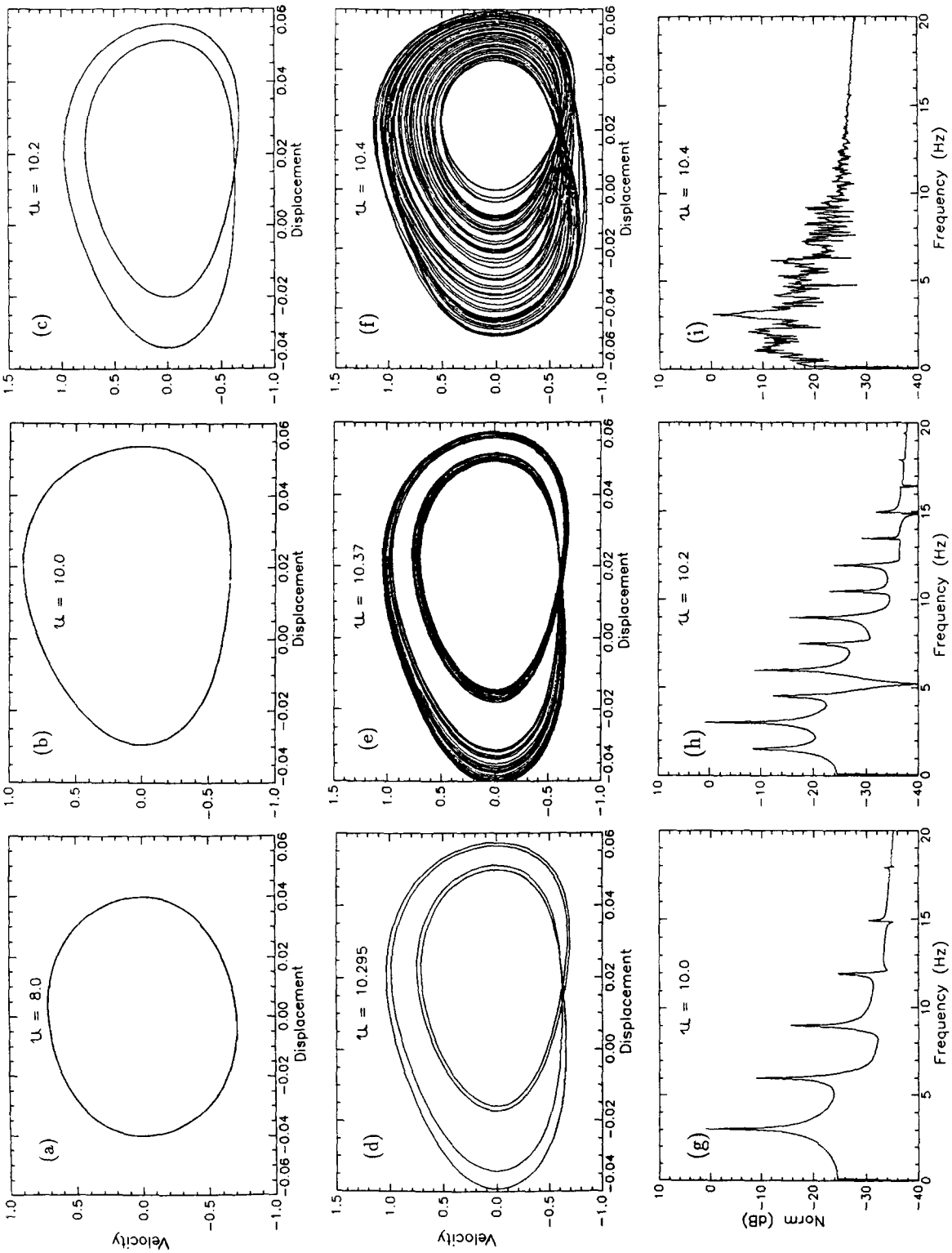

Fig. 3. Phase portraits and power spectra for $N = 2$, $\kappa = 10^5$, $\xi_b = 0.75$, $\beta = 0.213$, $\gamma = 26.75$, $\alpha = 5 \times 10^{-3}$, and different values of u.

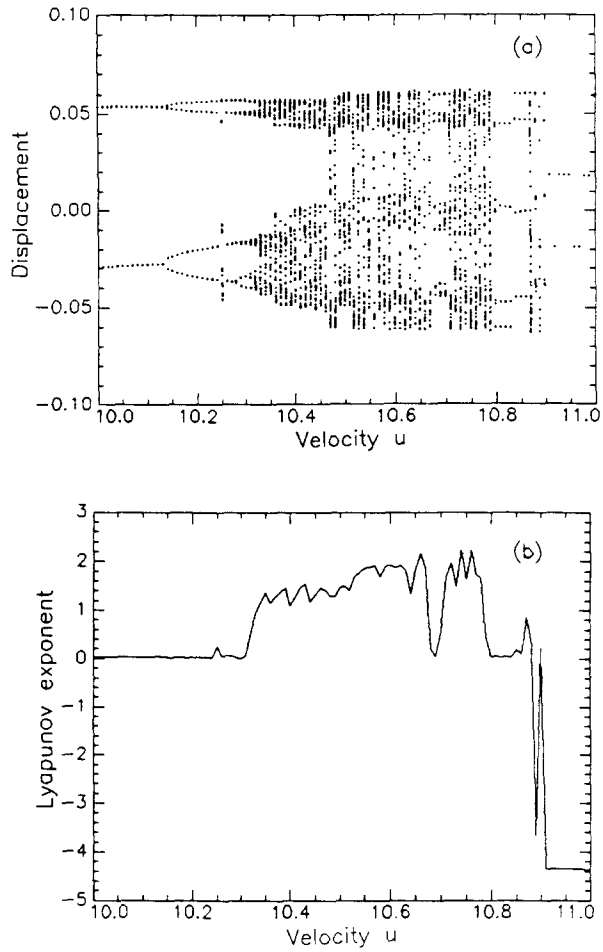

Fig. 4. (a) Bifurcation diagram for the $N = 2$ model: the tip (end) displacement as a function of the flow velocity u; (b) Lyapunov exponents, also as a function of u; $\kappa = 10^5$, $\xi_b = 0.8$, $\beta = 0.18$, $\gamma = 26.75$, $\alpha = 5 \times 10^{-3}$.

ment and the Lyapunov exponents σ are plotted as functions of the flow velocity u (Figure 4(a,b)). For the autonomous system, $\sigma < 0$ represents stable equilibria, $\sigma = 0$ corresponds to periodic oscillations and $\sigma > 0$ to chaotic motions [17].

It is observed that, after the region of chaos, the system 'regains stability', the solutions being attracted to a new stable equilibrium point. This corresponds exactly to experimental observations: for higher flow velocities, beyond the chaotic regions, the system attaches itself permanently to one of the constraints; i.e., the system becomes unstable by divergence. This clearly appears in the bifurcation diagrams as well as in Figure 5. The oscillations are periodic for $u = 10.82$ and are overdamped for even higher flow velocities (Figure 5(a)). An investigation of the existence of fixed points indicates that a subcritical saddle-node bifurcation occurs at $u = 9.85$; two fixed points exist beyond that value of u: one of them stable, and the other one unstable [18]. The computation of their respective eigenvalues leads to the conclusion that the stable fixed point becomes 'more and more' stable when u increases (Figure 4 and 5(b)), until finally it becomes the strongest limit set in the system. By setting initial conditions close to the stable equilibrium, the detection of the fixed points is possible, even within the chaotic regions (Figure 5(c)). Hence, different attractors coexist all along.

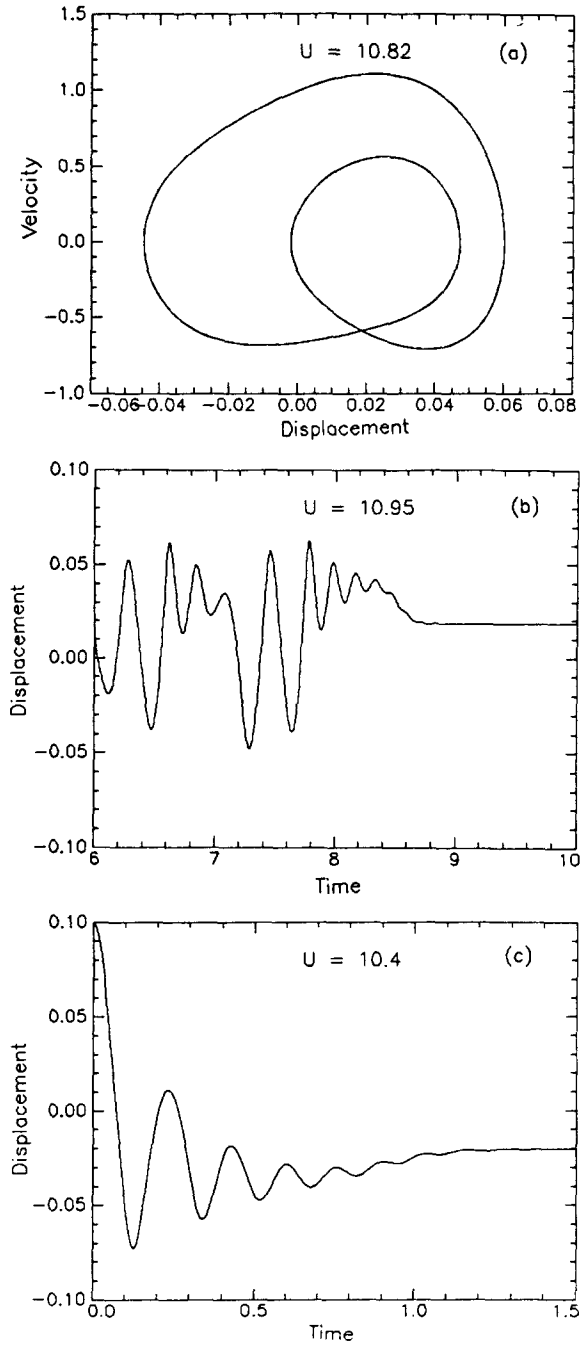

Fig. 5. Corresponding phase portrait and time traces showing (a) periodic oscillations beyond the chaotic region at $u = 10.82$; (b) static instability beyond the chaotic and periodic regions at $u = 10.95$; (c) existence of a stable fixed point in the chaotic region for $u = 10.40$.

3.2.2. $N = 2$ and Smoothed Trilinear Restraints

Similar bifurcation diagrams and phase plots were constructed, but without giving more new insight of the problem. Therefore, the results will be discussed, without any additional figures

being given.

First, it is interesting to note that for $\xi_b = 0.8$, a bifurcation diagram similar to the one shown in Figure 4 is found, but with lower nondimensional flow velocities u. Indeed, in this case, denoting by pf and pd the pitchfork and the period-doubling bifurcations, one finds $u_{pf} = 7.6$ and $u_{pd} = 7.75$, while chaotic oscillations occur at $u_{ch} = 8.0$. These values are lower than in the case of the cubic spring. Moreover, an inspection of the influence of the impact location ξ_b proves that for $u = 8.7$, chaotic motions occur only in the range $0.75 < \xi_b < 0.82$ (for $\xi_b < 0.75$ the system oscillates and for $\xi_b > 0.82$ it converges to one of the stable fixed points). Qualitatively, this has been observed in the experiments. However, for $\xi_b = 0.65$, which is the experimental value, chaos does not occur; this shows that, in the case $N = 2$, the better model of the impact forces does not improve very much the thresholds at which period-doubling or chaos may occur.

3.2.3. Concluding Remarks for the $N = 2$ Model

The principal findings of this series of calculations were three. First, the nonlinear terms in the equation of motion play a very important role, to the extent of invalidating some of the qualitatively attractive results obtained earlier with the linearized equation (always apart of the nonlinear constraint term). Second, it is now possible to conduct simulation with realistic values of the spring constraint ($\kappa = \mathcal{O}(10^5)$), and the limit-cycle amplitudes are now quite reasonable. Third, bifurcation diagrams with ξ_b as a variable were constructed (since experimentally the location of the constraints may be varied very easily), and the cascade of period-doubling bifurcations was observed, followed by a 'static restabilization', confirming the qualitative agreement with the experiments of the nonlinear $N = 2$ model. However, it is not possible to find chaotic oscillations for the experimental $\xi_b = 0.65$. Finally, with the parameter values close to the experimental ones (except for ξ_b), the $N = 2$ model generates critical values for the various bifurcations which are fairly close to those observed experimentally.

3.3. Three- and Four-Degree-of-Freedom Models ($N = 3$ or 4)

Based on the quite reasonable and promising results obtained with the $N = 2$ system with the experimental parameter values, it was fully expected that the results with $N = 3$ would be similar, and perhaps closer to the experimental values. However, the dynamical behaviour in this case was much more complex and less close to the experiments. A typical bifurcation diagram for the case of a cubic spring is shown in Figure 6(a), where it is seen that, beyond the pitchfork bifurcation (occurring at $u = 9.25$), rather than obtaining the usual cascade of period-doubling bifurcations, the amplitude of the oscillations decreases until the oscillations finally die out for $u = 10.4$. Therefore, for $u > 10.4$, the system settles down to one of the stable equilibrium points. It should be mentioned that the asymmetry due to the pitchfork bifurcation has been kept in Figure 6(a), but if opposite initial conditions had been used, the other part of the curve could have been obtained very easily.

It ought to be remarked that similar atypical results had been obtained for $N = 3$ in the study by Païdoussis *et al.* [11], utilizing the linearized equation of motion; they were in the original paper but were eventually left out because of space limitations.

However, the results for Figure 6(b), obtained with a smoothened trilinear spring, are less atypical and much more reasonable, both qualitatively and quantitatively. Period-doubling is

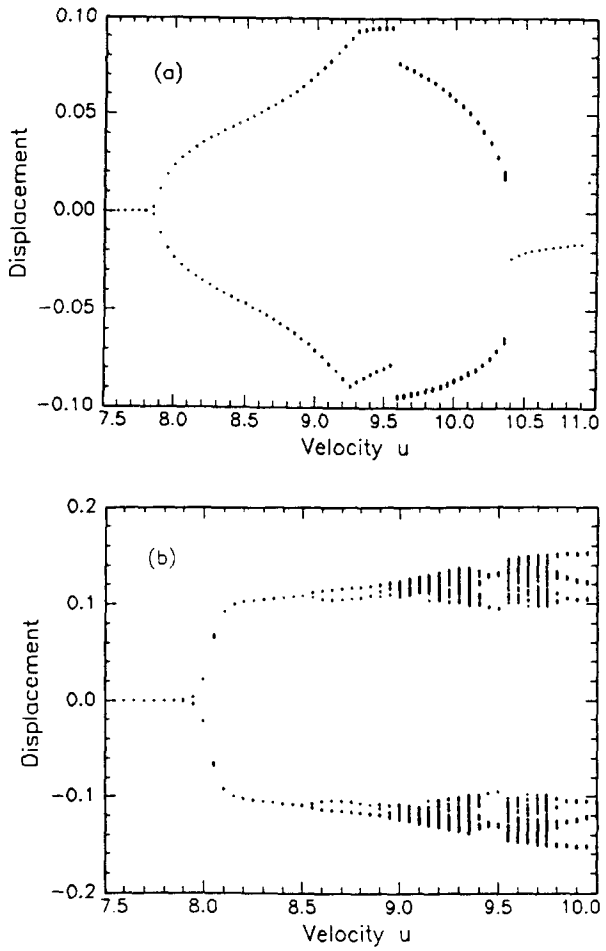

Fig. 6. Bifurcation diagram for the $N = 3$ model with (a) the cubic spring and (b) the trilinear representation of the constraints. All other parameters are adjusted to the experimental ones (see Section 3.1).

obtained at $u = 8.8$ and chaos at $u = 9.2$. Nevertheless, a complete qualitative agreement with the experiments is not achieved since no restabilization can be found. Different configurations have been tried to obtain this static restabilization (using for example the Kelvin–Voigt representation or different constraint configurations [11]), but no better agreement was obtained.

The reason why $N = 3$ gives such atypical results is not understood. Perhaps it should be mentioned that physically discrete, articulated systems also display a discontinuous 'convergence' in terms of increasing N for $N = 2$ and 3 [19]; for $N > 3$, on the other hand, the convergence to the continuous system – cf. the results obtained here to the $N = \infty$ case – is smooth.

Calculations were performed also with $N = 4$ for the case of a trilinear representation of the restraint stiffness. As expected again, very good agreement, both qualitatively and quantitatively, is achieved. First period-doubling bifurcation and chaotic oscillations occur at $u_{pd} = 9.1$ and $u_{ch} = 9.2$, respectively (Figure 7(a)) – cf. values in (8). After a range of velocity for which periodic oscillations are observed ($9.35 < u < 9.55$), stronger chaotic motions appear again ($u = 9.6$) in Figure 7(b), and for $u > 9.7$, the system settles down onto

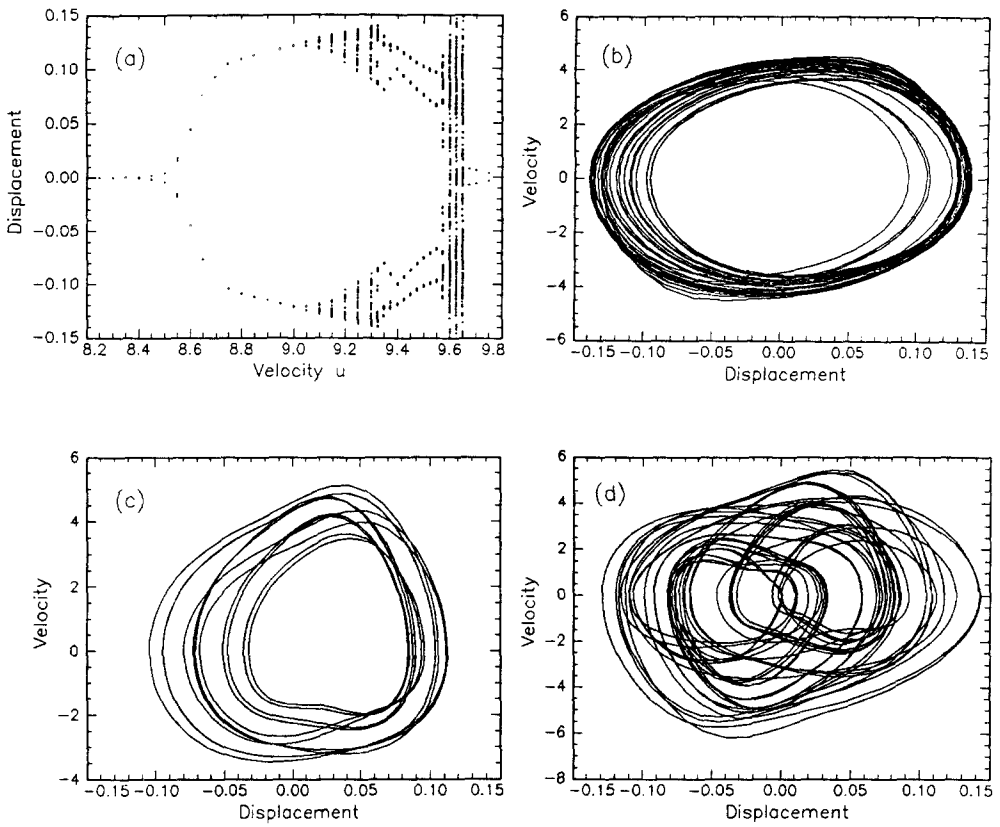

Fig. 7. (a) Bifurcation diagram and (b–d) some corresponding phase portraits for the $N = 4$ model and the trilinear representation of the constraints. All other parameters are adjusted to the experimental ones (see Section 3.1). For (b) $u = 9.3$, (c) $u = 9.57$, (d) $u = 9.6$.

one of the constraints. This is exactly what has been observed experimentally.

Again, many configurations have been tested for $N = 4$. For viscous damping ($\alpha = 0.005$) the same qualitative bifurcation diagram was obtained, with $u_{pd} = 8.6$, $u_{ch} = 9.0$ and static restabilization at $u_{re} = 9.7$, while for another impact model, $u_{pd} = 8.95$, $u_{ch} = 9.2$ and $u_{re} = 9.65$ were found. Therefore, the maximum difference with the experimental values is less than 8%.

It should be mentioned that in the case $N = 4$, almost no difference among the critical velocities u was found when the intrinsic nonlinear terms were removed. The static restabilization however was then not observed, which leads to the conclusion that the nonlinear terms still play an important role in the dynamics of the system.

As seen in Table 1, the results for $N = 4$ appear to be close to convergence. This compares well with the results obtained by Païdoussis *et al.* [11], which is meaningful, in view of the observation made in the previous paragraph; in [11], convergence was found to have been achieved between $N = 4$ and $N = 5$. This conclusion of convergence *circa* $N = 4$ is further reinforced by noting that the Hopf bifurcation limit cycle has nondimensional amplitude of ~ 0.1 for $N = 3$ and ~ 0.12 for $N = 4$; the corresponding maximum amplitudes for chaos are 0.15 in both cases.

Table 1. Convergence of nondimensional flow velocities, u, for the key bifurcations; subscripts *H, pd, ch* and *re* stand for *Hopf, period doubling, chaos* and *restabilization* (divergence), respectively.

	$N = 3$	$N = 4$	*Experimental*
u_H	7.95	8.40	8.04
u_{pd}	8.90	9.05	8.43
u_{ch}	9.20	9.20	8.72
u_{re}	10.35	9.65	~ 9.0

4. Conclusion

In this paper, the effect of the nonlinear terms in the equation of motions on the dynamics of a constrained cantilevered pipe conveying fluid was explored. However, more broadly, this is a multidimensional investigation of the effects of (i) the aforementioned nonlinearities (of the type associated with large motions), (ii) the number of degrees of freedom in the modelling of the system, and (iii) the impact model for the motion constraints.

Of course, this is a very specific problem, and this study can be justified only in terms of the more general conclusions that are reached concerning the analytical modelling of nonlinear systems when trying to match experimentally observed behaviour. Such questions as the effect of selective straining of parameters to give 'good agreement' in some sense, how easy it is to misinterpret the reasons for 'failure' of an analytical model, the fragility versus robustness of the theoretically predicted behaviour, etc., are some of the aspects of this study that *are* of generic interest. The problem at hand, may then be considered simply as a vehicle in the exploration of some of these questions, in the sense of the previous paragraph. Having said that, however, there is no question that the study of large-amplitude-related nonlinearities in the equation of motions of the specific problem under consideration had to be studied, in order to complete the circle of studies of References [7, 9–11] – e.g., to remove any suspicion that the excellent agreement between theory (without these nonlinear terms) and experiment achieved by Païdoussis *et al.* [11] may have been fortuitous.

It is shown that one can 'force' the system to some extent, by straining (relaxing) some of the physical parameters, to yield dynamical behaviour which is qualitatively similar to that observed – and with reasonable quantitative prediction of some of this behaviour. This was achieved with the $N = 2$ models, with a cubic-spring representation of the constraints [7, 8]: if the values for constraint location (ξ_b) and spring stiffness (κ) were strained, critical flow velocities for the bifurcations (Hopf, period-doubling, onset of chaos) could be predicted remarkably well. Admittedly, some other aspects of the predicted behaviour are then unrealistic, e.g., the amplitudes of limit-cycle motion.

It is of interest that the straining in the values of ξ_b and κ ($N = 2$ model) was *forced* on the investigators involved [7, 9] by the fact that no convergent solutions could be obtained for the correct values. One of the findings of this paper is that the reasons supposed to be responsible ($N = 2$, instead of higher N) were erroneous: once the nonlinear terms are included in the

equations of motion, then convergent solutions with the correct κ *are* possible. Thus, one of the main conclusions of this paper is that the nonlinear terms in the equation of motions, despite 'small motions' being modelled, can have an important effect on system dynamics – the extent of which cannot be gauged *a priori.* Moreover, as more realism is introduced (e.g. in the modelling of the constraint stiffness), the model can be tightened up to predict (i) realistic amplitudes of motion, (ii) the hitherto never predicted new equilibrium resulting (in the experiments) in the 'sticking' of the pipe to one of the constraints at sufficiently high flow velocities, u, (iii) critical u for the important bifurcations reasonably close to the experimental ones.

One looks at the behaviour of the system in the multidimensional parameter space, and hence the 'section' of the dynamics for $N = 2$, and at the changes occurring as nonlinear terms are included or κ is increased, and so on. Hence, the model $N = 2$ can be considered fragile. Therefore, it is essential to look at other 'sections', notably for higher-dimensional models (corresponding to $N > 2$), to probe the robustness of the analytical model, since dimension calculations have shown that to be able to capture the essential behaviour of the system, $N = 4$ or 5 would be needed [10], as confirmed by the excellent agreement obtained even when the nonlinear terms in the equations of motion were absent [11]. It is shown here that the inclusion of the nonlinear terms, although it still has an effect on the dynamics, otherwise *improves* the agreement between theory and experiment, by (i) being able to predict the static restabilization (sticking) observed experimentally at high u, (ii) predicting more realistic amplitudes, while (iii) not having a detrimental effect on the excellent agreement between experimental and theoretical values of u [11] for the key bifurcations (Hopf, period-doubling, *et seq.*). Equally interestingly, the number of parameters that need to be strained and the degree of straining are greatly diminished when the full nonlinear equation is used, even with $N = 2$. For $N = 4$, the degree of agreement with experiment becomes excellent, with *zero* straining of the parameters when the full nonlinear equation is used. More importantly, it is shown that the behaviour of the system is now very robust, and small excursions in this part of the parameter space have little effect on the predicted dynamics of the system.

The final conclusion is something that has been known for some time: one should be chary of 'good agreement' between observed and modelled behaviour, unless all aspects of the analytical model and its robustness have been looked into. This study documents one such case where the initial model was in a fragile parameter sub-space, but the final, modified model is very robust and capable of predicting well almost all essential aspects of the observed dynamical behaviour.

Acknowledgements

The authors express their appreciation to the Natural Sciences and Engineering Research Council of Canada and Le Fonds FCAR of Québec for supporting this research.

References

1. Païdoussis, M. P., 'Pipes conveying fluid: a model dynamical problem', *in Proceedings of Canadian Congress of Applied Mechanics*, Winnipeg, Man., Canada, 1991, 1–33; also in *Journal of Fluids and Structures* **7**, 1993, 137–204.
2. Holmes, P. J., 'Bifurcations to divergence and flutter in flow-induced oscillations: a finite-dimensional analysis', *Journal of Sound and Vibration* **53**, 1977, 471–503.
3. Lundgren, T. S., Sethna, P. R., and Bajaj, A. K., 'Stability boundaries for flow-induced motions of tubes with an inclined terminal nozzle', *Journal of Sound and Vibration* **64**, 1979, 553–571.

4. Rousselet, J. and Herrmann, G., 'Dynamic behavior of continuous cantilevered pipes conveying fluid near critical velocities', *Journal of Applied Mechanics* **43**, 1981, 945–947.
5. Bajaj, A. K., Sethna, P. R., and Lundgren, T. S., 'Hopf bifurcation phenomena in tubes carrying a fluid', *SIAM Journal of Applied Mathematics* **39**, 1980, 213–230.
6. Tang, D. M. and Dowell, E. H., 'Chaotic oscillations of a cantilevered pipe conveying fluid', *Journal of Fluids and Structures* **2**, 1988, 263–283.
7. Païdoussis, M. P. and Moon, F. C., 'Nonlinear and chaotic fluidelastic vibrations of a flexible pipe conveying fluid', *Journal of Fluids and Structures* **2**, 1988, 567–591.
8. Païdoussis, M. P. and Issid, N. T., 'Dynamic stability of pipes conveying fluid', *Journal of Sound and Vibration* **33**, 1974, 267–294.
9. Païdoussis, M. P., Li, G. X., and Moon, F. C., 'Chaotic oscillations of the autonomous system of a constrained pipe conveying fluid', *Journal of Sound and Vibration* **135**, 1989, 567–591.
10. Païdoussis, M. P., Cusumano, J. P., and Copeland, G. S., 'Low-dimensional chaos in a flexible tube conveying fluid', *Journal of Applied Mechanics* **59**, 1992, 196–205.
11. Païdoussis, M. P., Li, G. X., and Rand, R. H., 'Chaotic motions of a constrained pipe conveying fluid: comparison between simulation, analysis and experiment', *Journal of Applied Mechanics* **58**, 1991, 559–565.
12. Semler, C., Li, G. X., and Païdoussis, M. P., 'The nonlinear equations of motion of a pipe conveying a fluid', accepted for publication in the *Journal of Sound and Vibration*, 1992.
13. Païdoussis, M. P. and Semler, C., 'Nonlinear dynamics of a fluid-conveying cantilevered pipe with an intermediate spring support', *Journal of Fluids and Structures* **6**, 1992, 269–298.
14. Semler, C., 'Nonlinear dynamics and chaos of a pipe conveying fluid', Master's Thesis, Faculty of Engineering, McGill University, 1991.
15. Gregory, R. W. and Païdoussis, M. P., 'Unstable oscillation of tubular cantilevers conveying fluid. I. Theory; II. Experiments', *Proceedings of the Royal Society (London), Series A* **293**, 512–527 and 528–542.
16. Tousi, S. and Bajaj, A. K., 'Period-doubling bifurcation and modulated motions in forced mechanical systems', *Journal of Applied Mechanics* **57**, 1985, 446–452.
17. Moon, F. C., *Chaotic Vibrations: An Introduction for Applied Scientists and Engineers*, Wiley, New York, 1987.
18. Iooss, G. and Joseph, D. D., *Elementary Stability and Bifurcation Theory*, Springer Verlag, New York, 1981.
19. Païdoussis, M. P. and Deksnis, E. B., 'Articulated models of cantilevers conveying fluid: the study of a paradox', *I. Mech. E. Journal of Mechanical Engineering Science* **12**, 1970, 288–300.